GSI Annual Report 2012 (extracts)

TASCA

Theory

Miscellaneous

The Superheavy Element Search Campaigns at TASCA

J. Khuyagbaatar[1,2], A. Yakushev[1], Ch.E. Düllmann[1,2,3], H. Nitsche[4], J. Roberto[5], D. Ackermann[1], L.-L. Andersson[2], M. Asai[6], H. Brand[1], M. Block[1], D.M. Cox[7], M. Dasgupta[8], X. Derkx[2,3], A. Di Nitto[3], J. Dvorak[2], K. Eberhardt[2,3], P.A. Ellison[4], N.E. Esker[4], J. Even[2,3], M. Evers[8], C. Fahlander[9], U. Forsberg[9], J.M. Gates[4], N. Gharibyan[10], K.E. Gregorich[4], P. Golubev[9], O. Gothe[4], J.H. Hamilton[11], D.J. Hinde[8], W. Hartmann[1], R.-D. Herzberg[7], F.P. Heßberger[1,2], J. Hoffmann[1], R. Hollinger[1], A. Hübner[1], E. Jäger[1], J. Jeppsson[9], B. Kindler[1], S. Klein[3], I. Kojouharov[1], J.V. Kratz[3], J. Krier[1], N. Kurz[1], S. Lahiri[12], B. Lommel[1], M. Maiti[12], K. Miernik[5], S. Minami[1], A. Mistry[7], C. Mokry[2,3], J.P. Omtvedt[13], G.K. Pang[4], P. Papadakis[7], I. Pysmenetska[1], D. Renisch[3], D. Rudolph[9], J. Runke[1], K. Rykaczewski[5], L.G. Sarmiento[9], M. Schädel[1,6], B. Schausten[1], D.A. Shaughnessy[10], A. Semchenkov[13], J. Steiner[1], P. Steinegger[14], P. Thörle-Pospiech[2,3], E.E. Tereshatov[10], T. Torres De Heidenreich[1], N. Trautmann[3], A. Türler[14], J. Uusitalo[15], D. Ward[9], N. Wiehl[2,3], M. Wegrzecki[16], V. Yakusheva[2]

[1]GSI, Darmstadt, Germany, [2]HIM, Mainz, Germany, [3]U. Mainz, Germany, [4]LBNL+UC Berkeley, CA, USA, [5]ORNL / UT Knoxville, USA, [6]JAEA Tokai, Japan, [7]U. Liverpool, UK, [8]ANU, Canberra, Australia, [9]Lund U. Sweden, [10]LLNL, USA, [11]Vanderbilt U, USA, [12]SINP, Kolkata, India, [13]U. Oslo, Norway, [14]U. Bern+PSI Villigen, Switzerland, [15]U. Jyväskylä, Finland, [16]ITE Warsaw, Poland

Successful experiments on the synthesis of elements with Z=114-118 in ^{48}Ca-induced reactions with actinide targets were first performed at the DGFRS in Dubna [1]. Results for Z=114 (Fl) and Z=116 (Lv) nuclei have been later on confirmed by other groups [2-4].

Using doubly-magic ^{48}Ca for the synthesis of yet heavier elements is not possible due to the lack of sufficient amounts of target materials for elements beyond Cf. Thus, several attempts to produce element 120 in reactions with projectiles beyond ^{48}Ca have been carried out at DGFRS and SHIP [5-7]. The separator TASCA and its detection systems were significantly upgraded since the experiment on ^{288,289}Fl [3] was performed [8]. In the past two years, two experiments on the synthesis of elements beyond Z=118 have been undertaken at TASCA using the reactions ^{50}Ti + ^{249}Bk $\rightarrow$ ^{299}119* and ^{50}Ti + ^{249}Cf $\rightarrow$ ^{299}120*. To verify the performance of the setup, element 117 was also synthesized.

The first attempt to form element 120 at TASCA was performed in August-October 2011. The search for element 119 was performed in two series from April to September 2012. The beam energies from the UNILAC, average initial target thicknesses (*d*) [9], and accumulated beam doses for each reaction are given in Table 1. These values are **preliminary**. Beam doses were deduced from beam current measurements in front of the target. 85% of the beam doses were estimated to be on the target.

Subsequent to the months-long experiments on elements 119 and 120, an experiment on the synthesis of element 117 in reaction ^{48}Ca + ^{249}Bk $\rightarrow$ ^{297}117* was successfully performed. In about one month of experiment time, the Bk target was bombarded by ^{48}Ca ions at three different beam energies. The final data analyses of all these experiments are currently ongoing.

We are grateful for support by the GSI directorate, ion source, accelerator, and experiment electronics staff.

References

[1] Y. Oganessian, Radiochim. Acta 99, 429 (2011)
[2] L. Stavsetra *et al*., PRL. 103, 132502 (2009)
[3] Ch.E. Düllmann *et al*., PRL. 104, 252701 (2010)
[4] S. Hofmann *et al*., EPJ. A 48, 62 (2012)
[5] S. Hofmann *et al*., GSI Scientific Report-2007, 131 (2008)
[6] Yu.Ts. Oganessian *et al*., PRC. 79, 024603 (2009)
[7] S. Hofmann *et al.*, GSI Scientific Report-2011, 205 (2012)
[8] see GSI Scientific Report-2011, pages-206, 212, 217, 218, 251-253 (2012)
[9] J. Runke *et al*., J. Radioanal. Nucl. Chem. (accepted)

Table. 1. The parameters of the experiments. For details, see text.

Beam	Target	CN	Date	E_{lab} (MeV)	*d* (μg/cm^2)	Beam dose	Beam dose on target
^{50}Ti	^{249}Cf	^{299}120	25.08-12.10.2011	306	515	1.1·10^{19}	0.9·10^{19}
	^{249}Bk	^{299}119	13.04-03.07.2012 23.07-03.09.2012	300	440	4.2·10^{19}	3.6·10^{19}
^{48}Ca		^{297}117	26.09-09.10.2012	270		0.6·10^{19}	0.5·10^{19}
			09.10-22.10.2012	274		0.5·10^{19}	0.4·10^{19}
			22.10-29.10.2012	268		0.3·10^{19}	0.2·10^{19}

Superheavy Element Flerovium is the Heaviest Volatile Metal

A. Yakushev[1], J.M. Gates[1,2†], A. Gorshkov[1], R. Graeger[1], A. Türler[1‡], D. Ackermann[2], M. Block[2], W. Brüchle[2], Ch.E. Düllmann[2,3], H.G. Essel[2], F.P. Heßberger[2,3], A. Hübner[2], E. Jäger[2], J. Khuyagbaatar[2,3], B. Kindler[2], J. Krier[2], N. Kurz[2], B. Lommel[2], M. Schädel[2], B. Schausten[2], E. Schimpf[2], K. Eberhardt[4], M. Eibach[4], J. Even[4], D. Hild[4], J.V. Kratz[4], L.J. Niewisch[4], J. Runke[4], P. Thörle-Pospiech[4], N. Wiehl[3,4], J. Dvorak[5,6], H. Nitsche[5,6], J.P Omtvedt[7], A. Semchenkov[7], U. Forsberg[8], D. Rudolph[8], J. Uusitalo[9], L.-L. Andersson[10], R.-D. Herzberg[10], E. Parr[10], Z. Qin[11], M. Wegrzecki[12]*

[1]TUM, Garching, Germany; [2]GSI, Darmstadt, Germany; [3]HI Mainz, Germany; [4]University of Mainz, Germany; [5]LBNL, Berkeley, USA; [6]University of California, Berkeley, USA.; [7]University of Oslo, Norway; [8]Lund University, Sweden; [9]University of Jyväskylä, Finland; [10]University of Liverpool, UK; [11]IMP, Lanzhou, P.R. China, [12]ITE, Warsaw, Poland

Electron shells of superheavy elements (SHE), i.e., elements with atomic numbers $Z \geq 104$, are influenced by strong relativistic effects caused by the high value of Z. Early atomic calculations for element 112 (copernicium, Cn) and element 114 (flerovium, Fl) predicted them to have closed and quasi-closed electron shell configurations, respectively, and to be noble gas-like due to very strong relativistic effects [1]. Recent fully relativistic calculations studying Cn and Fl in different environments suggest them to be less reactive compared to their lighter homologues in the groups, but still exhibiting metallic character (see, e.g., [2]). Experimental gas-chromatography studies on Cn have, indeed, revealed a metal-metal bond formation with gold [3]. In contrast to this, for Fl, the formation of a weak physisorption bond with gold was inferred from first experiments [4].

A gas chromatography experiment on Fl at TASCA was conducted subsequently to the study of the reaction ^{244}Pu(^{48}Ca; 3,4n)^{289,288}Fl [5]. The coupling of chemistry setups to a recoil separator promises extremely high sensitivity due to strong suppression of background from unwanted species. TASCA was operated in the Small Image Mode, focusing the products into a Recoil Transfer Chamber (RTC) of 29 cm^3, from where they were flushed within 0.8 s to a detection setup (Fig. 1). Two COMPACT detectors [6] connected in series were used; each detector consisted of 32 pairs of 1x1 cm^2 PIN diodes covered with a 35 nm gold layer. The first detector was connected directly to the RTC exit and kept at room temperature.

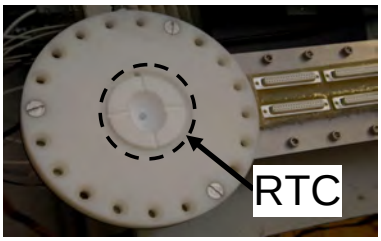

Fig.1: First COMPACT with the attached RTC.

A negative temperature gradient from +20 to −162 °C (Fig. 2, panel a) was applied in the second detector channel placed downstream to the first one. The use of two detectors in series allowed the detection of species in a wide volatility range – from the non-volatile Pb, the nearest homolog of Fl in the group, to the noble gas Rn. Two decay chains, one from ^{288}Fl and one ^{289}Fl were detected. Both decays from Fl isotopes occurred in the first detector channel at room temperature. The positions of decay chain members are shown in Fig. 2 (e) together with the Monte Carlo simulated deposition peak for ^{285}Cn (dashed line). Distributions of Pb, Hg, and Rn (Fig. 2, b-d) are also shown for comparison. The observed behavior of Fl in the chromatography column is indicative of Fl being less reactive than Pb. The evaluated lower limit of the adsorption enthalpy on gold reveals formation of a metal-metal bond with Au, which is at least as strong as that of Cn, and thus demonstrates the metallic character of Fl.

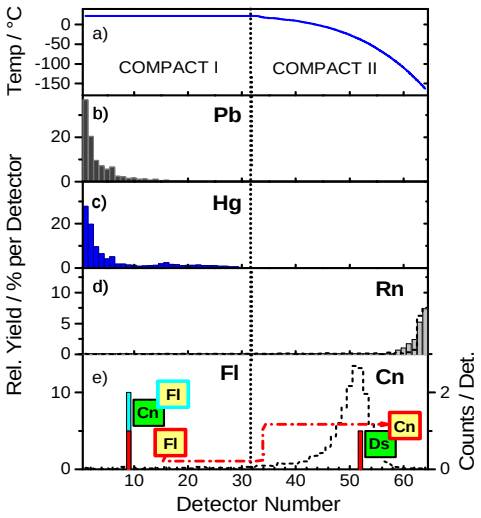

Fig. 2: The observed gas-chromatography behavior of Fl and Cn in COMPACT compared to those of Pb, Hg and Rn.

[1] K.S. Pitzer. *J. Chem. Phys.* **63**, 1032 (1975).
[2] V. Pershina *et al. J. Chem. Phys.* **131**, 084713 (2009).
[3] R. Eichler *et al. Nature* **447**, 72-75 (2007).
[4] R. Eichler *et al. Radiochim. Acta* **98**, 133-139 (2010).
[5] Ch.E. Düllmann *et al.* PRL **104**, 252701 (2010).
[6] J. Dvorak *et al.* PRL **97**, 242501 (2006).

* Current address: GSI Darmstadt, Germany
† Current address: LBNL, Berkeley, USA
‡ Current address: PSI, Villigen & Uni Bern, Switzerland

The reactions ^{50}Ti+^{206,208}Pb studied at TASCA

J. Khuyagbaatar[1,2], A. Yakushev[1], D. Ackermann[1], L.-L. Andersson[2], M. Block[1], Ch.E. Düllmann[1,2,3], J. Even[2,3], F.P. Heßberger[1,2], A. Hübner[1], E. Jäger[1], B. Kindler[1], J.V. Kratz[3], J. Krier[1], N. Kurz[1], B. Lommel[1], J.P. Omtvedt[4], J. Runke[1], M. Schädel[1,5], B. Schausten[1], J. Steiner[1], A. Türler[6], J. Uusitalo[7], N. Wiehl[2,3], V. Yakusheva[2]

[1]GSI, Darmstadt, Germany, [2]HIM, Mainz, Germany, [3]U. Mainz, Germany, [4]U. Oslo, Norway, [5]JAEA Tokai, Japan, [6]U. Bern+PSI Villigen, Switzerland, [7]U. Jyväskylä, Finland

Cross sections of the 1n and 2n evaporation channels of the complete fusion reactions ^{50}Ti + ^{206,208}Pb were measured. Selected beam energies correspond to the known or expected maxima of the 1n and 2n excitation functions. Evaporation residues (ER) were separated from the primary beam by TASCA [1] and implanted into a stop detector consisting of two double-sided silicon-strip detectors (DSSD). Two signals from the DSSD were read out and processed in analog (front strips) and digital electronics (back strips) as described in [2].

Rf isotopes were identified in a correlation analysis between the ER implantation signal and the subsequent radioactive decay (alpha emission or/and spontaneous fission (SF)).

Half-lives were deduced from the measured time distributions (see Fig. 1) and agree well with literature values [3]. Time distributions of the correlated alpha or/and SF decays of these isotopes are shown in Fig. 1 together with fits of the universal time distribution function [4].

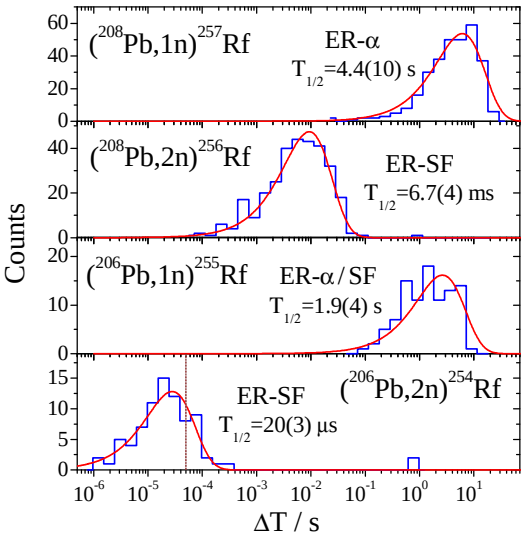

Fig 1: Time distribution of α/SF decays of $^{254-257}$Rf. The dotted line indicates the minimum readout time of the combined DAQ system.

Both analog and digital data were evaluated for the identification of short-lived ^{254}Rf.

The analog energy *vs.* correlation time plot for ER-SF correlations is shown in Fig. 2a. This energy is the uncorrected pulse height recorded in the stop detector, applying a calibration with an external α-source. Traces of two SF events (circled in Fig. 2a) are shown in Fig. 2b as illustrative examples. The energies recorded by the analog electronics were 94 and 150 MeV. In the digital part both traces saturate due to the pre-amplified SF signals, which are higher than the input voltages of the sampling ADC. However, the saturation time, T$_{sat}$, can be related to the SF energy. A typical trace of an ER correlated with a short-lived SF is shown in Fig. 2c. Such digital data were exploited in the analysis of ^{254}Rf data given in Fig. 1. Note that such events result in a single ER event in the analog electronics and fast decays of ^{254}Rf would be lost.

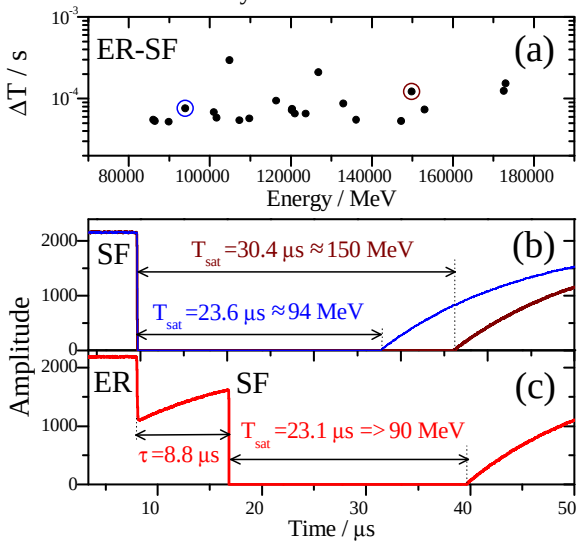

Fig 2: (a) Energy *vs.* correlation time plot. (b) Two traces of SF events selected from the analog ER-SF correlations. (c) Trace of an ER followed by a short-lived SF.

The cross section values for ^{50}Ti(^{208}Pb,1-2n)^{256,257}Rf and ^{50}Ti(^{206}Pb,2n)^{254}Rf were in agreement with the values measured at SHIP [5]. The cross section around the expected maximum for the ^{50}Ti(^{206}Pb,1n)^{255}Rf excitation function was measured for the first time. The data are currently under final analysis.

References

[1] A. Semchenkov *et al.*, NIM. B 266, 4153 (2008)
[2] J. Khuyagbaatar *et al.*, GSI Scientific report (2012)
[3] http://www.nndc.bnl.gov/ensdf/
[4] K.H. Schmidt *et al.*, Z. Phys. A 316, 19 (1984)
[5] F. P. Heßberger *et al.*, Z. Phys. A 359, 415 (1997)

Carbonyl Complex Formation of Short-Lived Ir and Re Isotopes*

J. Even[1#], A. Yakushev[2], Ch.E. Düllmann[1,2,3], J. Dvorak[1], R. Eichler[4], O. Gothe[5], D.Hild[3], E. Jäger[2], J. Khuyagbaatar[1,2], J.V. Kratz[3], J Krier[2], L. Niewisch[3], H. Nitsche[5], I. Pysmenetska[3], M. Schädel[2,7], B. Schausten[2], A. Türler[4,6], N. Wiehl[1,3], D. Wittwer[4,6]

[1]HIM, Mainz, Germany, [2]GSI, Darmstadt, Germany; [3]University Mainz, Mainz, Germany; [4]PSI, Villigen, Switzerland, [5]LBNL, Berkeley, CA, USA; [6]University of Bern, Bern, Switzerland; [7]JAEA, Tokai, Japan

We recently reported on the in-situ carbonyl complex formation of short-lived group 6 and group 8 elements [1]. These elements are well known to form mononuclear, volatile carbonyl complexes. However, no mononuclear, binary complexes of group 7 and 9 elements are known from literature (see e.g. [2]). We studied the transport of short-lived Ir and Re isotopes in a He-CO atmosphere, which gives a hint at the formation of volatile carbonyl complexes of these elements.

In first experiments at the TRIGA reactor in Mainz, the transport of fission products of the neutron induced fission of ^{249}Cf in a CO containing gas-stream was studied. The transported isotopes were collected on a charcoal filter and measured with a γ detector. Volatile fission products as well as short-lived isotopes of the refractory elements Mo, Tc, Ru and Rh were identified. However, precursor effects prevent a clear assignment to the transported element. To get a better understanding, the homologs Re and Ir were produced in ^{24}Mg-induced fusion reactions with ^{nat}Eu and ^{nat}Tb targets at the gas-filled separator TASCA. The recoiling isotopes were separated from the primary beam and transfer products in TASCA and thermalized in the recoil transfer chamber in a He-CO atmosphere. The volatile species were transported in the gas stream through a 10-m long capillary to a charcoal filter which was monitored by a γ detector. This way the transport of $^{178-179}$Ir and $^{170-172/172m}$Re was observed. Both, Re and Ir, apparently form volatile complexes with CO under these experimental conditions.

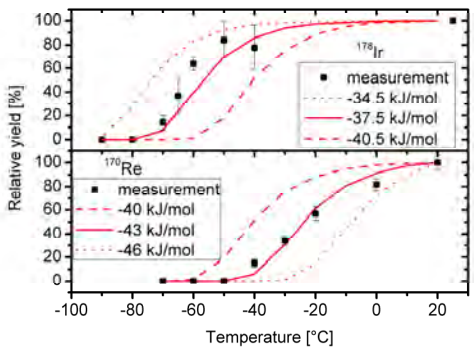

Figure 1: Transport yield of Re and Ir depending on the temperature of the isothermal chromatography column. The lines show results of Monte Carlo Simulations.

* Work supported by the Helmholtz Institute Mainz, the Research Center Elementary Forces and Mathematical Foundations (EMG), the BMBF under contract No. 06MZ223I, and the Swiss National Science Foundation under contract No. 200020 126639 #j.even@gsi.de

In further investigations the adsorption and decomposition of these complexes were studied. In the adsorption-studies on a quartz surface, the gas-stream was guided through an isothermal quartz column. The temperature was varied from measurement to measurement and the transport yield through the column was determined for each temperature. These measurements were modeled with Monte Carlo Simulations, which yield values for the adsorption enthalpy of these complexes on the quartz surface. For the Re complexes the adsorption enthalpy was determined to be (−43 ± 3) kJ/mol, and for the Ir ones (−37.5 ± 3.0) kJ/mol. Figure 1 shows the breakthrough curves and the results of the Monte Carlo Simulations. The thermal stabilities of these compounds were studied by passing the gas stream through a quartz wool plug heated by an oven before reaching the charcoal filter. The transport yields were determined for various temperatures. (see Figure 2) The complexes start to decompose at temperatures around 300°C.

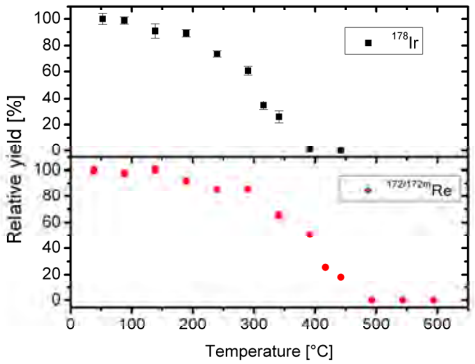

Figure 2: Transport yield of Re and Ir vs. the temperature of the quartz wool plug in the decomposition setup.

The experimental observation of the transport of Re and Ir in a CO-containing gas stream gives a hint on the formation of volatile complexes in CO. Further studies are planned to elucidate the nature of these complexes, which might open the door for bohrium and meitnerium chemistry experiments.

References

[1] J. Even et al., Inorg. Chem. **51**, 6431-6433 (2012).
[2] H. Werner, Angew. Chem. Int. Ed. **29**, 1077-1089 (1990).

High Intensity TASCA Target Wheel Control System and Target Monitoring

E. Jäger[1], H. Brand[1], Ch.E. Düllmann[1,2,3], J. Khuyagbaatar[1,3], J.Krier[1], M. Schädel[1], T. Torres[1], A. Yakushev[1]

[1]GSI Helmholtzzentrum für Schwerionenforschung GmbH, Darmstadt, Germany; [2]Johannes Gutenberg-Universität Mainz, Mainz, Germany; [3]Helmholtz-Institut Mainz, Mainz, Germany

The gas-filled recoil separator TASCA [1], optimized for actinide-target based hot fusion reactions, was recently used for studies of superheavy elements with Z = 115,117 and for the search for new elements [3,4]. These experiments require transuranium targets made from isotopes that are produced in high-flux nuclear reactors and are available only in very limited amounts [5-7]. At the GSI Darmstadt, the UNILAC provides intense beams, delivered with a 25% duty cycle (5 ms pulse length, 50 Hz repetition rate). Due to small cross sections for the production of the heaviest elements, maximum beam intensities are applied, which in turn put a large heat load onto the target.

At TASCA, a new target wheel has recently been developed [8], which was optimized for maximum applicable beam intensities, respecting the available amounts of target material, the desired areal density of 0.5 mg/cm^2, the maximum permissible beam spot size of 8 mm diameter, and the beam macrostructure. This new target wheel rotates at 2250 rpm and consists of four individual target segments with 6 cm^2 area each, necessitating about 12 mg of target material (Figure 1). Each beam pulse illuminates one single target, which subsequently cools during 75 ms before being hit by the next pulse. The target wheel is placed inside a target cassette. Upstream of the target wheel, a second wheel can be mounted, e.g., containing carbon stripper foils to increase the charge state of the beam.

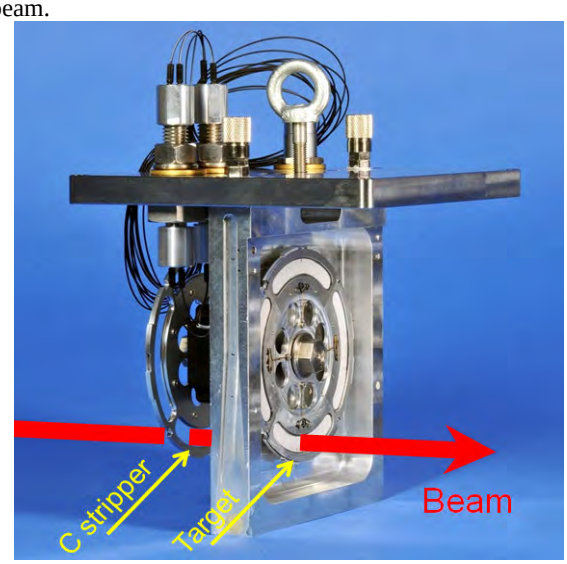

Figure 1. Photograph of the new TASCA target wheel.

The wheels are driven by a stepper motor (Nanotec). The wheel position control is provided by a microcontroller SPS and an industrial PC, which use signals from 2 photodiodes outside the target chamber connected to the target cassette through light fibers. This allows synchronizing the wheel rotation with the beam macrostructure such that each individual macro pulse illuminates a single target segment.

To insure target integrity, several on-line as well as off-line monitoring possibilities are exploited. The on-line control is a part of the "TASCA Control System" (Figure 2) and is based on a beam current measurement and a contact-free temperature measurement of the beam-spot area with a pyrometer. Upon violation of user-defined thresholds, or asynchronous rotation, the beam is switched off within 1 µs. Off-line capabilities include the monitoring of the target and the carbon stripper foil wheel with two endoscopes, which allows obtaining sets of 36 pictures covering all four segments. If the target isotope has a significant α branch, the α particles can be guided to the focal plane detector in TASCA, where the rate of incoming α particles and the energy spectra yield information on the target thickness and status of the layer.

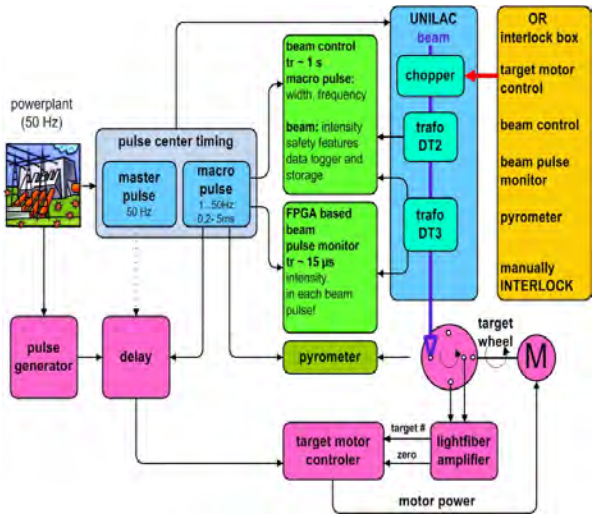

Figure 2. Scheme of on-line target monitoring system.

[1] A. Semchenkov et al., NIMB 266 (2008) 4153
[2] J.M. Gates et al., PRC 83 (2011) 054618
[3] J. Khuyagbaatar et al., This GSI Annual Report.
[4] U. Forsberg, Acta Phys. Pol. B 43 (2012) 305.
[5] J.E. Bigelow et al., ACS Symp. Ser. **161**, 3-18 (1981).
[6] K. Eberhardt et al., NIMA 590, 134-140(2008).
[7] J. Runke et al., J. Radioanal. Nucl. Chem. (in print).
[8] E. Jäger et al., J. Radioanal. Nucl. Chem. (in print)

Ab initio Studies of Atomic Properties and Experimental Behavior of element 119 and Its Lighter Homologs

A. Borschevsky[1], V. Pershina[2], E. Eliav[3], and U. Kaldor[3]
[1]Helmholtz Institute Mainz, Mainz D-55128, Germany; [2]GSI, Darmstadt, Germany; [3] Tel Aviv University, Israel

We performed relativistic benchmark calculations of the polarizabilities (α) of element 119 and its lighter homologs, Cs and Ra, and their cations. Besides being of theoretical interest in the context of atomic studies of heavy and superheavy elements, these properties are also important for prediction of adsorption enthalpy (ΔH_{ads}) of the atoms on inert surfaces, which is required to guarantee the transport of the newly produced element from the target chamber to the chemistry set up.

The polarizabilities were calculated using the finite field approach [1]. The energy calculations were performed within the Dirac-Coulomb (DC) Hamiltonian,

$$H_{\mathrm{DC}} = \sum_i h_D(i) + \sum_{i<j} 1/r_{ij}.$$

Here, h_D is the one electron Dirac Hamiltonian,

$$h_D(i) = c\boldsymbol{\alpha}_i \cdot \mathbf{p}_i + c^2\beta_i + V_{nuc}(i),$$

where α and β are the four dimensional Dirac matrices. The nuclear potential V_{nuc} takes into account the finite size of the nucleus, modelled by a Gaussian distribution.

Electron correlation was taken into account at the relativistic coupled cluster level, including single, double, and perturbative triple excitations (RCCSD(T)). The uncontracted Faegri basis set [2] was used for the three atoms and extended to convergence with respect to the calculated polarizabilities. The final basis sets were 26*s*23*p*16*d*8*f*4*g* for Cs, 26*s*23*p*18*d*13*f*6*g*2*h* for Fr, and 29*s*26*p*20*d*15*f*6*g*2*h* for element 119. All the calculations were performed using the DIRAC08 computational package [3].

Based on the calculated polarizabilities and other atomic properties and using a physisorption model given by Eq. (6) of Ref. 4, we estimate the ΔH_{ads} of group-1 elements on a Teflon surface. The van der Walls radii (R_{vdW}) were determined from a linear correlation between the known R_{vdW} in Group 1 [5] and the radii of the maximal charge density (R_{max}) of the valence *ns* orbitals [6].

Table 1.Polarizabilities of neutral (α(M)) and singly charged (α(M^+)) group-1 elements (a.u.), and their R_{vdW} (Å) and ΔH_{ads} (kJ/mol) on Telfon. All the values were calculated here, unless reference otherwise.

	Na	K	Rb	Cs	Fr	119
α(M)	162.7[a]	290.6[a]	318.8[a]	399.0	311.5	169.7
α(M^+)	1.0[b]	5.5[b]	9.1[b]	15.5	20.1	31.6
R_{vdW}	2.27[c]	2.75[c]	2.90	3.16	3.09	2.78
$-\Delta H_{ads}$	32.7	29.3	26.6	24.6	21.2	17.6

[a] Exp., Ref. [7]; [b] Theor., Ref. [8]; [c] Exp., Ref. [5]

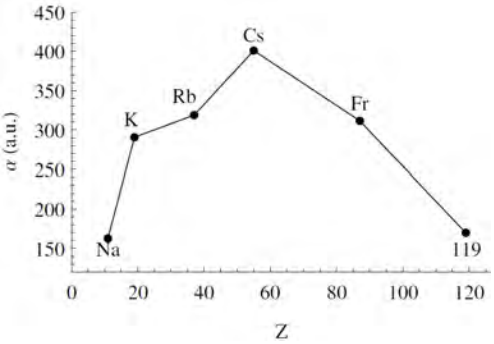

Figure 1. Polarizabilities of group-1 elements

The calculated α, R_{max}, and ΔH_{ads} of group-1 elements are presented in Table I. The obtained α of Cs is in excellent agreement with the experimental value (401.0±0.6 [9]); similar accuracy can be expected from our predictions for Fr and element 119. For the neutral atoms, α (Fig. 1) and R_{vdW} increase from Na to Cs and then decrease towards element 119, which can be explained by the strong relativistic contraction of the valence *ns* orbital in the heavier atoms in the group. In fact, the same trend reversal at Cs is also observed for the ionization potentials and electron affinities of group-1 atoms, discussed in Ref. 10. In case of the cations, a different trend in the polarizability is observed, defined by the outer $(n\text{-}1)p_{3/2}$ orbital, which expands in the group with the increase in the atomic number. Thus, 119^+ will have the highest polarizability of group-1 cations. The $-\Delta H_{ads}$ in the group decrease with the increase in the atomic number, and the predicted $-\Delta H_{ads}$ of element 119 on Teflon is the lowest among the atoms considered here, as is the case with its $-\Delta H_{ads}$ on noble metals [10] . The low value of 17.6 kJ/mol indicates that this atom should be easily transported through the Teflon capillaries to the chemistry set up.

References

[1] U. Kaldor, J. Phys. B **6**, 71 (1973)
[2] K. Faegri, Theor. Chim. Acta **105**, 252 (2001)
[3] DIRAC08, written by H. J. Ja. Jensen *et al*. (2008)
[4] V. Pershina and T. Bastug, Chem. Phys. **311**, 139 (2005)
[5] A. Bondi, J. Phys. Chem. **68**, 441 (1964)
[6] J. Desclaux, At. Data Nucl. Data Tables **12**, 311 (1973)
[7] V. Holmgen *et al.*, Phys. Rev. A **89** 053607 (2010)
[8] I.S. Lim *et al.*, J. Chem. Phys. **116**, 172 (2002)
[9] J. M. Amini and H. Gould, Phys. Rev. Lett. **91**, 153001 (2003)
[10] V. Pershina *et al.*, Chem. Phys. **395**, 87 (2012)

Theoretical Predictions of Properties and Gas-Phase Behaviour of Carbonyl Complexes of Group-6 Elements Cr, Mo, W, and Element 106, Sg

V. Pershina[1] and J. Anton[2]
[1]GSI, Darmstadt, Germany; [2]Institut für Elektrochemie, Universität Ulm, Germany.

Up to now, experimental gas-phase chemical studies were performed for elements 104 (Rf) through 108 (Hs), 112 (Cn) and 114 (Fl) [1]. A search for a new class of volatile species suitable for gas-phase chromatography studies resulted in the idea to synthesize carbonyl complexes of the heaviest elements. Accordingly, carbonyl complexes of Mo, W and Os, homologs of Sg and Hs, respectively, were synthesized and studied on their volatility by using both the isothermal (IC) and thermochromatography (TC) techniques [2].

Theoretical predictions of gas-phase properties and chromatography behaviour of the heaviest elements and their homologs has been a subject of our long-term research [3]. In the present work, we predict properties of group-6 $M(CO)_6$ (M = Cr, Mo, W, and Sg) and their adsorption behaviour on quartz for future gas-phase chromatography experiments. For calculations, we used our 4-component, fully relativistic, Density Functional Theory method developed within the non-collinear spin-polarized formalism [4]. For calculations of the adsorption energy of the molecules on a neutral (quartz) surface, the following model for a molecule-slab interaction was used [5]:

$$E(x) = -\Delta H_{ads} = -\frac{3}{16}\left(\frac{\varepsilon-1}{\varepsilon+2}\right)\frac{\alpha_{mol}}{\left(\frac{1}{IP_{slab}}+\frac{1}{IP_{mol}}\right)x^3}$$

Here, ε is the dielectric constant of the surface material, IP_{mol} and IP_{slab} are ionization potentials of the molecule and surface material, respectively, α_{mol} is molecular polarizability and x is the molecule - surface interaction distance estimated using molecular bond lengths.

Results of the calculations of molecular properties (also in comparison with other calculations [6]) needed for predictions of adsorption are given in Tables 1 and 2.

Table 1. Calculated and experimental bond lengths, R_e (in Å), of $M(CO)_6$ (M = Cr, Mo, W, and Sg)

	Method	R_e(M-C)	R_e(C-O)
$Cr(CO)_6$	4*c*-DFT	1.913	1.152
	exp.	1.918	1.141
$Mo(CO)_6$	4*c*-DFT	2.067	1.152
	RECP CCSD(T)[a]	2.076	1.147
	exp.	2.063	1.145
$W(CO)_6$	4*c*-DFT	2.062	1.153
	RECP CCSD(T)[a]	2.065	1.148
	exp.	2.058	1.148
$Sg(CO)_6$	4*c*-DFT	2.123	1.154
	RECP CCSD(T)[a]	2.112	1.150

[a] Ref. [6].

Table 2. Ionization potentials, IP (in eV), average polarizabilities, α (in a.u.), molecule-surface adsorption distances, x (in Å), and adsorption enthalpies, $-\Delta H_{ads}$ (in kJ/mol), of $M(CO)_6$ (M = Cr, Mo, W, and Sg) on quartz

	IP	$<\alpha>$	x	$-\Delta H_{ads}$
$Cr(CO)_6$	9.07	133.24	2.695	45.4 ± 2.5
$Mo(CO)_6$	9.003	156.41	2.784	48.1 ± 2.5
				42.5 ± 2.5[a]
$W(CO)_6$	8.925	151.54	2.781	46.5 ± 2.5[b]
$Sg(CO)_6$	8.631	159.43	2.82	46.2 ± 2.5

[a] IC experiment [2]; [b] TC experiment [2].

The data show that the electronic structure of $Sg(CO)_6$ is very similar to those of the Mo and W homologs. Accordingly, its volatility should also be very similar to those of the lighter homologs (Table 2). Fig. 1 shows that, indeed, all the homologs will have similar, within the error bars, ΔH_{ads}(M) on quartz.

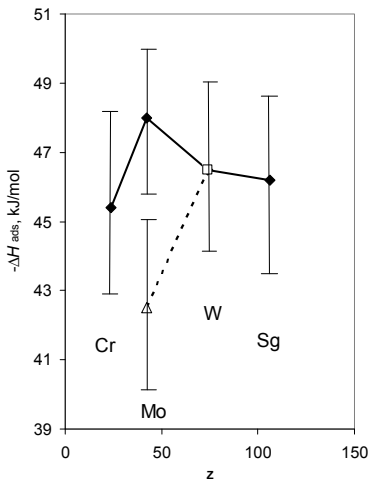

Fig. 1. Predicted (solid line) and measured (dashed line: the open rhomboid is the IC measurements; the open square is the TC ones [2]) adsorption enthalpies of $M(CO)_6$ (M = Cr, Mo, W, and Sg) on quartz.

References

[1] A. Türler and V. Pershina, Chem. Rev., in print
[2] J. Even, et al. Inorg. Chem. **51**, 6431 (2012).
[3] V. Pershina, Radiochim. Acta **99**, 459 (2011).
[4] J. Anton, et al., Phys. Rev. A **69**, 012505 (2004).
[5] V. Pershina and T. Bastug, Chem. Phys. **311**, 139 (2005)
[6] C. N. Nash, B. E. Bursten, J. Am. Chem. Soc., **121**, 10830 (1999).

Theoretical Predictions of Properties of Element 120 and its Adsorption on Noble Metal Surfaces

V. Pershina[1], A. Borschevsky[2] and J. Anton[3]
[1]GSI, Darmstadt, Germany; [2]HIM, Mainz, Germany; [3]Institut für Elektrochemie, Universität Ulm, Germany.

In the present work, we predict chemical properties and adsorption behaviour of element 120 whose production was attempted recently at the GSI, Darmstadt [1]. The most promising nuclear reaction appears to be ^{50}Ti + ^{249}Cf giving the ^{295}120 and ^{296}120 isotopes in the 4*n* and 3*n* evaporation channel, respectively [2]. Expected lifetime, of the order of μs, is too short for study of chemical properties of this element using current gas-phase chromatography techniques. However, development of vacuum chromatography could open new prospects in this field.

An analysis of atomic properties, calculated within the Dirac-Coulomb-Breit approach [3], shows that the relativistic stabilization and contraction of the valence ns AO in group 2 results in the inversion of trends beyond Ba, so that element 120 will be more electronegative than Ca. In this work, chemical reactivity of element 120 in comparison with its lighter homologs Ca through Ra was studied on the example of the M_2 and MAu dimers. Knowledge of properties of these compounds is indispensable for estimating quantities measured in the chromatography studies, i.e., sublimation, ΔH_{sub}, and adsorption enthalpies, ΔH_{ads}, on gold.

Molecular calculations were performed with the use of our fully relativistic, 4-component, Density Functional Theory method in the non-collinear spin-polarized approximation [4]. Results for M_2 and MAu are given in Tables 1 and 2, respectively.

Table 1. Spectroscopic properties of M_2 (M = K through element 120): bond lengths, R_e (in Å), dissociation energies, D_e (in eV) and vibrational frequencies, ω_e (in cm^{-1})[a]

Mol.	R_e	D_e	ω_e
Ca_2	4.236	0.141	66
	4.277	*0.137*	*65*
Sr_2	4.493	0.133	44
	4.498	*0.137*	*40*
Ba_2	4.831	0.226	43
Ra_2	5.193	0.106	25
$(120)_2$	5.646	0.018	9

[a] Values in italics are experimental.

The data of Table 1 show that $D_e(M_2)$ have a reversal of the trend beyond Ba. Thus, $(120)_2$ should be most weakly bound in the row of homologs, due to the 8s(120) AO contraction and van der Waals nature of bonding in M_2.

D_e(MAu) (Table 2) have also a reversal of the trend beyond Ba, so that 120Au should be the most weakly bound in the row of homologs due to the 8s(120) AO stabilization. ΔH_{sub} of the 120 metal and ΔH_{ads}(120) on gold were obtained via a correlation with the binding energies of the corresponding dimes in the group. According to the results, ΔH_{sub}(120) and -ΔH_{ads}(120) on Au (also on Pt and Ag) should be the smallest among the homologs.

Table 2. Properties of MAu (M = Ca through element 120): bond lengths, R_e (in Å), dissociation energies, D_e (in eV) and vibrational frequencies, ω_e (in cm^{-1})[a]

Mol.	R_e	D_e	ω_e
CaAu	2.627	2.706	221
	2.67	*2.545*	*221*
SrAu	2.808	2.629	159
BaAu	2.869	3.006	145
RaAu	2.995	2.564	105
120Au	3.050	1.902	97

[a] Values in italics are experimental.

Predicted trends in the adsorption of group-2 elements on noble metals are shown in Fig 1. The moderate values of ΔH_{ads}(120) are indicative of the feasibility of the chromatography chemical studies on this element.

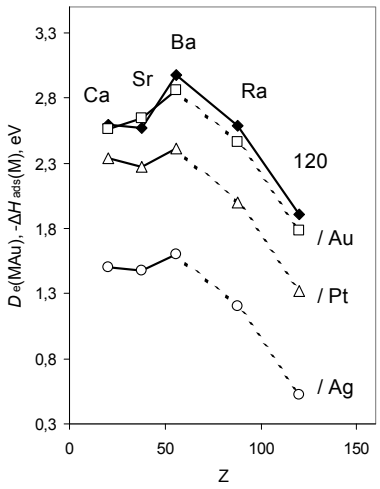

Fig. 1. Calculated D_e(MAu) (filled symbols) and -ΔH_{ads}(M) (open symbols), where M = Ca through element 120, on Au, Pt and Ag.

References

[1] Ch. E. Düllmann, et al., GSI Annual Report 2011.
[2] V. Zagrebaev and W. Greiner, Phys. Rev. C **78**, 034610 (2008).
[3] A. Borschevsky, et al. Phys. Rev. A, in print.
[4] J. Anton, et al., Phys. Rev. A **69**, 012505 (2004).

Spontaneous Fission Properties of ^{259}Sg and ^{255}Rf *

F.P. Heßberger[1,2], S. Antalic[3], D. Ackermann[1], M. Block[1,2], S. Heinz[1], S. Hofmann[1,4], Z. Kalaninová[3], I. Kojouharov[1], J. Khuyagbaatar[2,1], B. Kindler[1], B. Lommel[1], R. Mann[1]

[1]GSI, Darmstadt, Germany; [2]HIM, Mainz, Germany, [3]Comenius University, Bratislava, Slovakia, [4]Goethe Universität, Frankfurt a. Main, Germany

In a recent study decay properties of ^{259}Sg, produced in the reaction ^{206}Pb(^{54}Cr,n)^{259}Sg, were investigated at SHIP [1]. Alpha decay from two nuclear states in this isotope was observed: a) the ground state having a half-life of 411 ms and attributed to the Nilsson level 11/2$^-$[725]; b) an isomeric state located at $E^* \approx 92$ keV with a half-life of 254 ms, assigned as 1/2$^+$[620]. Search for spontaneous fission branches was rendered more difficult by the fact that the α-decay daughter ^{255}Rf has a fission branch of 52% and a half-life of 1.64 s [2]. Thus we searched for spontaneous fission events following the implantation of an evaporation residue (ER) within 10 s and not being preceded by an α-decay neither with full energy release nor with partial energy release in the focal plane detector. A probability $p_w < 0.05$ that a preceding α decay could have been missed and thus an sf event of ^{255}Rf wrongly assigned as an sf event of ^{259}Sg was estimated from the number of correlations α(^{259}Sg) – α(^{255}Rf) – α(^{251}No), α(^{259}Sg) – α(^{251}No) (without observation of α's of ^{255}Rf), and an ≈20% probability to observe only the escaping α-particle as obtained from α – γ - measurements.

Altogether 24 sf events not preceded by an α-decay were observed. Their time distribution (Δt(ER-sf)) is shown in fig. 1. A half-life $T_{1/2}$ = 235 $^{+62}_{-41}$ ms was obtained. As the half-life is in-line with that of the α activity attributed to the decay of the 1/2$^+$[620] level, the sf activity is also assigned to it. From the number of α decays and spontaneous fission events a branching ratio b_{sf} = 0.06±0.015 was obtained, resulting in a partial half-life of $T_{sf} \approx 3.9$ s. Our branching ratio is in-line with $b_{sf} \approx 0.11$, obtained from each one α-sf – correlation in decay studies of ^{263}Hs [3,4].

A hindrance of fission in nuclei having odd proton and/ or neutron numbers compared to neigbouring even-even nuclei is well known. The degree of hindrance can be expressed by a hindrance factor HF defined as HF = T_{sf}/T_{sf}(unh), with the partial fission half-life T_{sf} and the hypothetical 'unhindered' fission half-life T_{sf}(unh), usually obtained as the geometric mean of the fission half-lives of the neighbouring even-even nuclei [5]. Using the known values for the neighbours ^{258}Sg (2.6 ms) [6] and ^{260}Sg (7.0 ms) [7] we obtain T_{sf}(unh)(^{259}Sg) = 4.3 ms, and thus HF ≈ 907, which is about an order of magnitude lower than the value for the daughter ^{255}Rf.

Striking differences have also been observed for the measured 'fission energies', which are displayed in fig. 2. It should be noted, that the probability to stop both fission fragments in the focal plane detector is only 30%. So in most of the cases the observed 'fission energy' represents the sum of the kinetic energy of one fragment and the energy loss of the other fragment. We observed for ^{259}Sg an about 10% higher mean energy value and a narrower distribution of the fission energies than for ^{255}Rf. This is presently regarded as sign of two components in the mass distribution of the fission fragments of ^{255}Rf, but only one component in that of ^{259}Sg, i.e. a transition from asymmetric fission of ^{255}Rf to symmetric fission of ^{259}Sg.

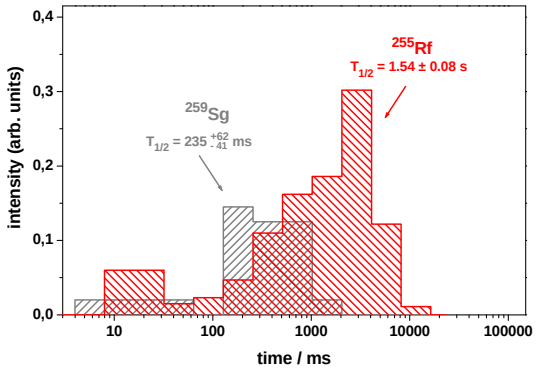

Figure 1: Time distributions Δt(ER-sf) of fission events not preceded by an α decay (^{259}Sg) and Δt(α-sf) of fission events preceded by an α decay (^{255}Rf)..

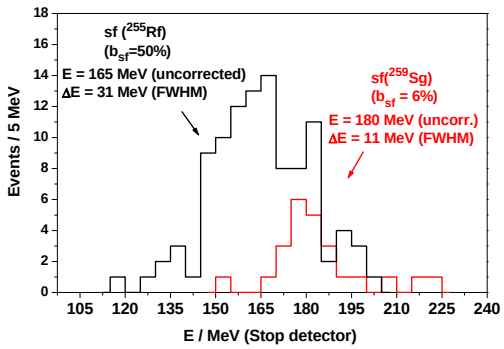

Figure 2: Energy distributions of fission events assigned to ^{255}Rf and ^{259}Sg. Given energy values are not corrected for pulse height defect.

References

[1] F.P. Heßberger et al. GSI Scientific Report 2011
[2] F.P. Heßberger et al. EPJ A 12, 57 (2001)
[3] I.Dragojevic et al. Phys.Rev.C79, 011602(R) (2008)
[4] D. Kaji et al. J. Phys. Soc. Japan 78, 035003 (2009)
[5] D.C. Hoffman Nucl. Phys. A 502, 21c (1989)
[6] F.P. Heßberger et al. Z. Phys. A 359, 415 (1997)
[7] F.P. Heßberger et al. EPJ A 41, 145 (2009)

* supported by HI Mainz

Chemistry for Isobar Separation behind SHIP*

J. Even[1#], D. Ackermann[2], M. Block[2], H. Brand[2], Ch.E. Düllmann[1,2,3], E. Jäger[2]; J. Khuyagbaatar[1,2], B. Kindler[2], J.V. Kratz[3], J. Krier[2], B. Lommel[2], F.P. Heßberger[1,2], J. Maurer[2]; J. Steiner[2], Th. Traut[3], N. Wiehl[1,3] and A. Yakushev[2]

[1]Helmholtz-Institut Mainz; Germany; [2]GSI, Darmstadt, Germany; [3]Johannes Gutenberg-Universität Mainz, Germany.

Recoil separators are powerful instruments for the isolation of desired nuclear reaction products. However, separation of ions of similar masses and isobaric nuclides is not possible at such a device without additional separation stages. One possibility for a second separation step is provided by chemistry. Two recoil separators at GSI are dedicated to superheavy element research – the velocity filter SHIP and the gas-filled separator TASCA. At gas-filled separators like TASCA, the coupling with chemistry setups is established[1]. In contrast, no vacuum separator has been used as a preseparator for chemical investigations so far. We have demonstrated that SHIP also can be combined with chemistry setups. Recently the in-situ formation of volatile metal carbonyl complexes was studied at TASCA [2,3]. Recoiling W, Re, Os, and Ir isotopes were thermalized in a CO containing atmosphere and formed volatile complexes. These complexes were transported in a gas jet over several meters to detection setups.

Short-lived Ta isotopes as well as Re and W isotopes were produced in the complete fusion reaction of ^{48}Ca projectiles with a ^{133}Cs^{127}I target at SHIP, in order to investigate the behaviour of Ta under comparable conditions. The Recoil Transfer Chamber (RTC), which was originally built for experiments at TASCA in the small image mode, was attached to SHIP. The chamber was separated from the high vacuum of SHIP by a 5.8-µm thick Mylar window supported by a honeycomb grid. The size of the RTC window was 3 cm × 4 cm. The chamber was cylindrical with an inner diameter of 3 cm. The depth of the RTC was 3 cm.

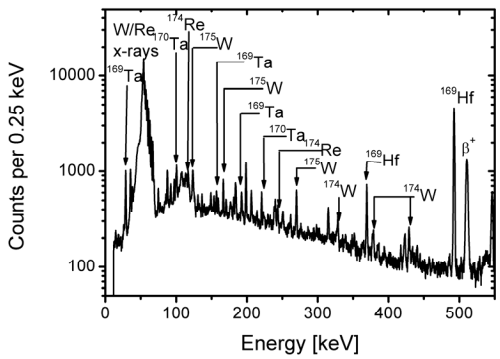

Figure 1: γ-spectrum of fusion products stopped in Al-foil behind SHIP.

In the first part of the experiment, an aluminium catcher foil was placed 5 mm behind the RTC window, where the recoiling ions were collected for 30 min. Within 2 min the foil was taken out of the RTC, placed in front of a γ detector, and measured for 10 min. Figure 1 shows a typical spectrum. γ-lines of ^{170,169}Ta produced in the reaction ^{127}I(^{48}Ca, 5-6n) and ^{174}Re produced in the reaction ^{133}Cs(^{48}Ca,7n) were observed. Furthermore ^{174,175}W and ^{169,170}Hf were identified. These are either produced in the (^{48}Ca,p xn)- reactions, or are decay products of the Re and Ta isotopes. In the second part of the experiment the catcher foils were removed, and the RTC was flushed with either a He/CO mixture or pure CO. The gases were purified by passing oxysorb and hydrosorb cartidges. The pressure in the RTC was kept at 600 hPa. The recoiling ions were thermalized in the RTC and all volatile compounds were transported in the gas stream out of the RTC through a 566 cm long capillary to a filter of activated charcoal. The volatile compounds adsorbed on the charcoal filter, which was monitored with the γ detector. Figure 2 shows a spectrum of the charcoal trap. Only W and Re isotopes were identified. No Ta and Hf isotopes were observed in the spectra.

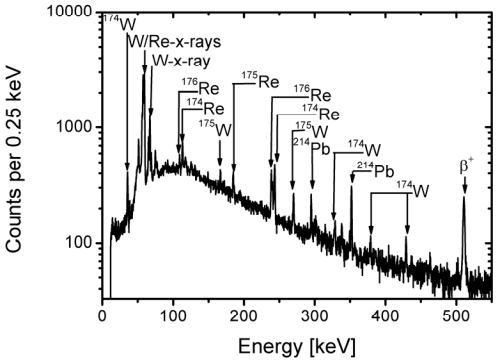

Figure 2: γ-spectrum of the charcoal filter. Pb γ-lines originate from the natural background.

This confirms former results that W and Re form volatile complexes in a CO atmosphere. However, Ta and Hf were not transported so that the formation of volatile complexes with CO was excluded. Gas phase carbonyl chemistry is therefore an appropriate tool to separate group 4 and 5 elements from group 6 and 7 elements and can thus be used for isobar separation.

References

[1] Ch.E. Düllmann et al., Radiochim. Acta **99** (2011), 515.
[2] J. Even et al., Inorg.Chem. **51**, (2012) 6431-6433.
[3] J. Even et al., this report.

* Work supported by the Helmholtz Institute Mainz, and the BMBF under contract No. 06MZ7165I,
#j.even@gsi.de

Preparation of ^{249}Bk targets

J. Runke[1], R.A. Boll[2], Ch.E. Düllmann[1,3,4], K. Eberhardt[3,4], B. Kindler[1], B. Lommel[1], C. Mokry[3], J.B. Roberto[2], K.P. Rykaczewski[2], P. Thörle-Pospiech[3], N. Trautmann[3], A. Yakushev[1]

[1]GSI Helmholtzzentrum für Schwerionenforschung GmbH, Darmstadt, Germany; [2]Oak Ridge National Laboratory, Oak Ridge, TN, USA; [3]Johannes Gutenberg-Universität Mainz, Germany; [4]Helmholtz-Institut Mainz, Germany

In the year 2012 two long experiments to synthesize the elements 119 and 117 have been performed at the gas-filled recoil separator TASCA at GSI. In both experiments ^{249}Bk was used as the target material, which was bombarded with ^{48}Ca for the synthesis of element 117 and ^{50}Ti to search for the new element 119.

For this, a ^{249}Bk target-wheel was used [1]. 12.7 mg ^{249}Bk in form of the nitrate were provided by Oak Ridge National Laboratory. The target segments were produced by Molecular Plating (MP) with high deposition yields at the Institute for Nuclear Chemistry at the University of Mainz [2,3].

The total amount of ^{249}Bk was delivered in four quartz vials covered with a Teflon septum. This septum was penetrated with a syringe containing 100 µl 0.1 M HNO_3 to dissolve the ^{249}Bk nitrate prior to the MP. After complete dissolution, the solution was transferred into the electrochemical deposition cell (EDC). The quartz vial was washed with 1 ml isopropanol and this solution was also transferred to the EDC. Finally 51 ml isobutanol were added.

The EDC [3,4] is made from polyether-etherketone (PEEK). On one side of the EDC, the target backing - a thin (~2 µm) Ti-foil produced by cold rolling and glued on an Al frame at the GSI Target Laboratory - was mounted and acted as the cathode. As an anode, a Pd-foil in the same geometry as the target frame was used. The EDC was clamped between two water cooled Ti blocks. For the mixing of the ^{249}Bk solution, an ultrasonic stirrer was applied. The deposition parameters for ^{249}Bk were similar to those for ^{249}Cf targets produced in 2011 [5], i.e., a current density of 0.3 mA/cm^2 was applied, resulting in voltages of 300 to 600 V. After deposition times of 3 to 4 hours target thicknesses of 354±18 – 508±25 µg/cm^2 with deposition yields exceeding 90 % were obtained.

The deposition yield and kinetics were determined by α-particle and γ-ray spectroscopy. Prior to the start of the deposition and then in one hour steps during the deposition, 10 µl aliquots of the supernatant solution were evaporated to dryness and measured by α-particle spectroscopy. Due to the rather short half-life of ^{249}Bk, its daughter, ^{249}Cf, is also present in the solution. Because both isotopes have α branches with significantly different α-particle energies, the deposition of both elements can be followed simultaneously in this way. The deposition kinetics of ^{249}Bk and ^{249}Cf are very similar. This allows the determination of the ^{249}Bk target thickness also via the γ-rays from ^{249}Cf, which is not possible for ^{249}Bk directly due to the absence of suitable γ-lines. For the determination of the deposition yield by γ-ray spectroscopy, a thin ^{249}Bk target was used as reference sample. The results of the yield determination by α-particle and γ-ray spectroscopy are in good agreement with each other. The average thickness of the target on the day of production was 463±23 µg/cm^2. The target segments were delivered to GSI and mounted on a target-wheel as shown in Fig. 1. The produced ^{249}Bk targets were able to resist a high total beam dose with beam intensities of over 4 particles microAmp for a long time.

Figure 1: ^{249}Bk target-wheel

Acknowledgments:
We are very thankful to the Oak Ridge National Laboratory for providing ^{249}Bk. The authors thank the Target Laboratory at GSI for providing the Ti-backing foils and the Mechanical Workshop of the Institute for Nuclear Chemistry in Mainz for the construction of the plating cells. This work was supported by the Helmholtz Institute Mainz.

References

[1] Jäger E, et al. (2012) submitted to J. Radioanal. Nucl. Chem.
[2] Eberhardt K, et al. (2008) Nucl. Instrum. Meth. Phys. Res. A 590:134-140
[3] Runke J, et al. (2012) submitted to J. Radioanal. Nucl. Chem.
[4] Haba H, et al. (2006) RIKEN Accel. Prog. Rep. 39:109
[5] Düllmann ChE, et al., GSI Sci. Rep. 2011 (2012), p. 206, PHN-NUSTAR-SHE-02

^{50}Ti for a High-Intensity Heavy-Ion Beam

Bettina Lommel[l], Andreas Beusch[1], Willi Hartmann[1], Annett Hübner[1], Birgit Kindler[1], Jutta Steiner[1], Vera Yakusheva[2,1]

[1]GSI, Darmstadt, Germany; [2] Helmholtz-Institut Mainz, 55099 Mainz, Germany

The semi-magic ^{50}Ti has a closed neutron shell with N = 28 and is the most neutron rich of the stable Ti-isotopes. This makes the isotope especially interesting as a beam projectile for heavy-element synthesis. For the production of a high intensity ion beam over long time periods, the metallic form of the enriched isotope is preferable for both, ECR and PIG ion sources.

Highly enriched ^{50}Ti is delivered either as the dioxide or as the tetrachloride. The task was to establish a process to reduce the compound to the metal with a high efficiency and a high chemical purity.

Process

For the reduction process we preferred the solid TiO_2 to the liquid $TiCl_4$ since handling gaseous $TiCl_4$ at higher temperatures needed for the reduction process involves a higher risk of losing material. For the TiO_2 there are in principle two common routes for reducing it to the metal either with metallic Ca or with CaH_2 as reducing agent [1]. Since for the affectivity of the reduction the purity of the Ca is crucial we decided to use the CaH_2 in the process. The Ca vapours are generated within the mixture via thermal decomposition of the hydride and can react immediately with the adjacent TiO_2.

The process chosen [2] is described by the following chemical equation:

$$TiO_2 + 2\ CaH_2 \rightarrow Ti + 2\ CaO + 2\ H_2 \uparrow \qquad (1)$$

For the reduction we prepared a mixture of the two components in an agate mortar with a 40% access of CaH_2 to the stoichiometric composition described by the reaction equation (1) and pressed to tablets with a hydraulic press. The tablets are heated in a molybdenum boat inside a stainless steel tube at 950°C for an hour in a constant flow of dry argon. After the reduction the tablets now containing Ti-metal, CaO and rest of Ca are cooled down to room temperature, dissolved in diluted acetic acid; then the precipitate is washed and dried, obtaining a fine powder of metallic Ti.

Analysis

At first the setup and the process were tested with different batches of natural TiO_2 where a yield of 95 % was achieved. For the application in the ion sources ten different batches of $^{50}TiO_2$ from three different producers were reduced. The starting material obviously differed in colour, in grain size and in softness leading to quite different behaviour by pressing tablets for the reduction and by melting metallic Ti, as well as a significantly variation in yield during reduction.

To get an understanding of the impurities in the starting material and their behaviour during the reduction process, energy-dispersive x-ray analysis (EDX) of all batches before and after the reduction was applied. In the natural material no impurities were detectable before the reduction, after the reduction a Ca-content of ~ 0.3 – 0.6 % was observed. Several batches of the enriched $^{50}TiO_2$ showed no impurities before and only the expected amount of calcium after the reduction. But a number of batches had impurities of Cl, Si or Sn or a combination of those. All impurities were in in the range of 1.5 % up to 5 %. The Cl vanished completely after the reduction, whereas the Si and the Sn stayed in the same amount.

The different impurities caused different behaviour in the further processing especially by melting tablet of Ti powder to beads.

Results

With the new setup we are able convert between 0.5 g up to several grams of highly enriched ^{50}Ti in one run with yields between 90 % and 98 %. Different impurities in the starting material influence the melting behaviour and therefore the final yield significantly. We obtain enriched metallic titanium for application in the ion source or as a starting material for target production. The reduced material was used at UNILAC for production of ^{50}Ti-beam with intensities of about 1 particleµA at a target for experiments which lasted several month in 2011 and 2012 [3,4,5].

References

[1] Handbuch der präparativen anorganischen Chemie (ed. G. Brauer) Ferdinand Enke Verlag, Stuttgart 1978, vol. 2

[2] W. Freundlich, M. Bichara, Comptes rendus hebdomadaires des séances de l'Académie des sciences / publiés par MM. les secrétaires perpétuels T238 (1954) p. 1324.

[3] K. Tinschert et al., this report.

[4] R. Hollinger, this report.

[5] B. Lommel, A. Beusch, W. Hartmann, A. Hübner, B. Kindler, J. Steiner, V. Yakusheva, J. Radioanal. Nucl. Chem. to be published.